

Comparative *in vivo* biodistributions of nanoparticles and polymers of ¹⁷⁷lutetium-labeled hyaluronic acids in mice during 28 days

Chunmei Lin^{1,2,†}, Ju-Yeon Jeong^{2,†}, Jung-Min Yon^{3,†}, Seul Gi Park², Lee Wha Gwon², Jong-Geol Lee², In-Jeoung Baek⁴, Sang-Soep Nahm⁵, Beom Jun Lee², Young Won Yun², Sang-Yoon Nam^{2,*}

¹College of Chinese Medicinal Materials, Jilin Agricultural University, Changchun 130118, China

²College of Veterinary Medicine and Veterinary Medical Center, Chungbuk National University, Cheongju 28644, Korea

³Division of Biosafety Evaluation and Control, Centers for Disease Control & Prevention, Cheongju 28159, Korea

⁴Asan Institute for Life Sciences, Asan Medical Center and University of Ulsan, Seoul 05505, Korea

⁵College of Veterinary Medicine, Konkuk University, Seoul 05029, Korea

(Received: February 21, 2017; Revised: May 14, 2017; Accepted: May 23, 2017)

Abstract: Hyaluronic acid (HA) has been investigated for biomedical and pharmaceutical applications. This study was conducted to determine the distributions of HA nanoparticles (NPs; size 350–400 nm) and larger HA polymers in mice at intervals after application. ¹⁷⁷Lutetium (Lu)-labeled HA-NPs or HA polymers were intravenously injected (5 mg/kg) into male ICR mice, and radioactivity levels in blood and target organs were measured from 0.25 h to 28 days post-injection. In blood, the radioactivities of HA-NPs and HA polymer peaked at 0.5 h after injection but were remarkably decreased at 2 h; subsequently, they maintained a constant level until 6 days post-injection. HA-NPs and HA polymers were observed in the liver, spleen, lung, kidney, and heart (in ascending order) but were seldom observed in other organs. After 3 days, both the HA-NP and HA polymer levels showed similar steady decreases in lung, kidney, and heart. However, in liver and spleen, the HA-NP levels tended to decrease gradually after 1 day and both were very low after 14 days, whereas the HA polymer level accumulated for 28 days. The results indicate that HA-NPs, with their faster clearance pattern, may act as a better drug delivery system than HA polymers, especially in the liver and spleen.

Keywords: drug delivery system, hyaluronic acid, *in vivo* biodistribution, nanoparticle, ¹⁷⁷lutetium

Introduction

There has been remarkable growth in the area of nanotechnology in recent years, and this field is expected to continue to bring noteworthy advances in the diagnosis and treatment of disease [10]. Molecular nanotechnology will provide great opportunities to improve the quality of human health services. Nanomedicine is expected to not simply be an extension of molecular medicine, but also help to solve medical problems using a molecular level of the mechanical system [21]. In fact, nanomaterial therapy improves intracellular penetration, facilitates absorption into selected tissues, increases clinical efficiency and reduces toxicity [19].

Drug delivery systems effectively deliver the minimum amount of a drug required for healing diseases by optimizing the efficiency and effectiveness and minimizing the side effects of existing medications [10]. Polymeric nanoparticles (NPs) have shown longer circulation and high accumulation

in tumor tissue after their intravenous administration, although the short stability of NPs in blood remains a critical obstacle to efficient tumor-targeted drug delivery [16]. To improve the stability of NPs, researchers have chemically crosslinked or mineralized NPs [13].

Hyaluronic acid (HA) is a polymer of disaccharides composed of D-glucuronic acid and D-N-acetylglucosamine linked via alternating β -1,4 and β -1,3 glycosidic bonds and is a polysaccharide polymer having more than 300 kDa molecular weight. HA, which is synthesized in the plasma membrane by a membrane-bound protein, can be very large, with its molecular weight often reaching the millions [12]. This compound is an important component of articular cartilage and skin. HA is also involved in the proliferation and motility of cells and participates in the receptor function of many cell surfaces such as its primary receptor, CD44 and receptor for HA mediated motility [2]. HA is degraded by a family of enzymes known as hyaluronidases. HA is used for a variety

*Corresponding author

Tel: +82-43-261-2596, Fax: +82-43-271-3246

E-mail: synam@cbu.ac.kr

†The first two authors contributed equally to this work.

of medical device applications including wound healing, eye surgery, arthritis, tendon repair, nerve guides, controlled drug release matrices, cosmetic applications, and dietary supplements for animals and humans [11].

Pharmacokinetic and organ distribution are important factors influencing novel NPs [3]. Nanomaterials may differ in toxicity and biodistribution depending on size; therefore, this study was conducted to evaluate the distribution and accumulation of HA-NPs and HA-polymers in the blood and tissues following intravenous application and to demonstrate the time-dependent fate of HA-NPs and HA-polymers in the animal body from 0.25 h to 28 days.

Materials and Methods

HA nanoparticles and polymers and animals

HA-polymers and HA-NPs were kindly provided by Dr. Kwangmeyung Kim of the Korea Institute of Science and Technology. The HA-NPs were spherical in shape and their sizes were in the range of 350 to 400 nm, depending on the degree of substitution of 5 β -cholic acid [8]. In this study, we administered ¹⁷⁷Lutetium labeled-HA-NPs and HA-polymers into an intravenous route frequently used in clinical application and confirmed *in vivo* pharmacokinetics and distribution by measuring the radioactivity in serum and organs over 28 days. Experiments were conducted using 7-week-old ICR mouse purchased from Central Lab. Animal (Seoul, Korea). ¹⁷⁷Lutetium (Lu)-labeled HA-NPs or HA-polymers were intravenously injected into ICR male mice (6 animals per group) at a single dose of 5 mg/kg for the investigation of their blood clearance and biodistribution in various time intervals of 0.5 h, 2 h, and 1, 3, 7, 14 and 28 days. All experiments were approved by the Chungbuk National University Animal Care Committee and conducted according to the Guide for Care and Use of Animals (CBNUA-608-13-01).

Radiolabeling of HA

¹⁷⁷Lu was produced in the HANARO research reactor installed in Korea Atomic Energy Research Institute (Korea) by the neutron irradiation of natural ¹⁷⁶Lu (n, γ)¹⁷⁷Lu. After the irradiation of a double capsulated ¹⁷⁶Lu₂O₃ target for several days at a neutron flux of 1.0×10^{14} n/cm², it was cooled for 48 h and dissolved in 3 mL of 0.05N HCl solution. After that, LuCl₃ (20 μ L, 5 mCi) solution diluted in 200 μ L of 0.05 N HCl solution and sodium acetate buffer (pH 5.5) were mixed with HA-NPs and HA-polymers in liquid state (1 mg/ μ L), after which was reacted for 15 min in room temperature or 50 °C water bath. It was confirmed by an instant thin layer chromatography whether ¹⁷⁷Lu was bound with HA in HCl solution and sodium acetate buffer solution in 50°C water bath. The radiolabeling yield, the radiochemical purity, and the stability of the ¹⁷⁷Lu-labeled HA-NAs and HA-polymers were determined by using a Cyclone Storage Phosphor System (Perkin Elmer, USA).

Measurement of radioactivity

We intravenously injected free ¹⁷⁷Lu to normal animals and then analyzed *in vivo* biodistribution using a gamma counter (Perkin Elmer) at 24 h after injection (data not shown). ¹⁷⁷Lu labeled-HA-NP and HA-polymer (5 mg/kg) were administered via the tail vein, after which the biodistribution was analyzed in blood and organs (liver, spleen, lung, kidney, and heart) at 0.5 h, 2 h, 1 day, 3 days, 7 days, 14 days and 28 days after intravenous injection. The radioactivity was measured using an ionizing chamber (Atomlab 200; Biodex, USA) by setting the calibration value for ¹⁷⁷Lu that was corrected and calibrated by the manufacturer. These series of experiments were conducted at the Korea Atomic Energy Research Institute (Korea).

Statistical assays

Means and standard errors (SEM) were calculated for the radioactivity of HAs from blood and organs at each evaluation interval. Statistical differences between groups were analyzed by one-way analysis of variance followed by Tukey's multiple comparison test. Statistical significance was established at $p < 0.05$. All analyses were conducted using SPSS for Windows, (ver. 23.0; SPSS, USA).

Results

Blood clearance

To understand the movement of degradable HA-NPs and HA-polymers in mice, we intravenously injected ¹⁷⁷Lu labeled-HA-NPs and HA-polymers into ICR mice at 5 mg/kg and measured the amount of the radioactivity remained in the blood at 0.25 h, 0.5 h, 1 h, 2 h, 1 day, 3 days and 6 days after

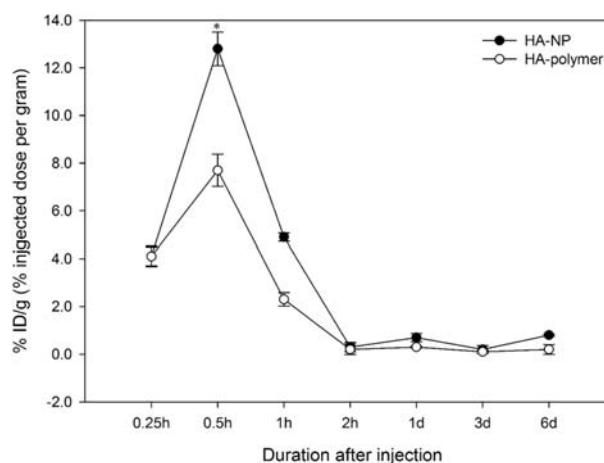


Fig. 1. Blood clearance of ¹⁷⁷lutetium (¹⁷⁷Lu)-labeled hyaluronic acid (HA)-nanoparticles (NPs) (●) and HA-polymers (○) after intravenous injection at different time periods. After intravenous injection, blood clearance peaked at 0.5 h after injection, then dramatically decreased, after which it was maintained at a similar level for 2 h after injection. Data are presented as injected dose per gram (%ID/g) and expressed as the mean \pm SEM ($n = 6$). * $p < 0.05$ between HA-NPs and HA-polymers.

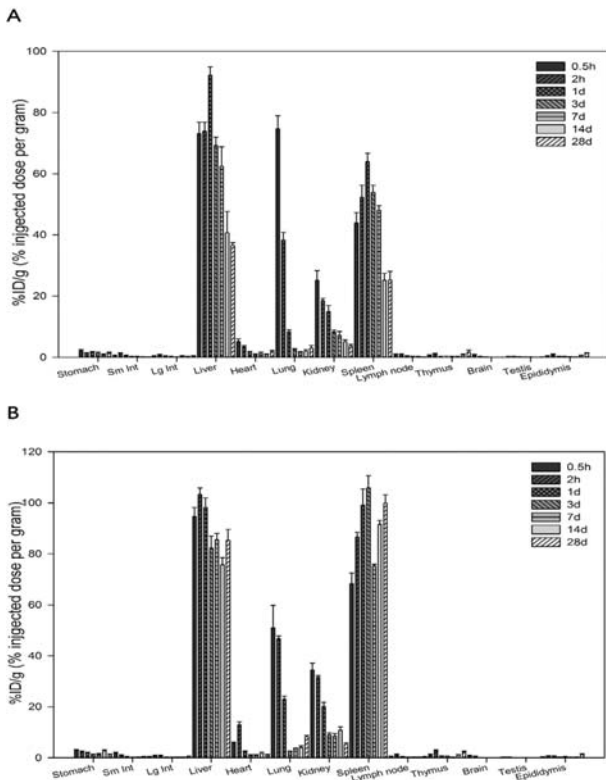


Fig. 2. Biodistribution of ¹⁷⁷Lu-labeled-HA-NPs (A) and ¹⁷⁷Lu-labeled-HA-polymers (B) in several organs. The materials were mostly found in the liver, spleen, lung, kidney, and heart. (A) HA-NPs distribution was high in the liver, spleen, lung, kidney, and heart sequence and (B) HA-polymers distribution was high in spleen, liver, lung, kidney, and heart sequence. Data are presented as injected dose per gram (%ID/g) and expressed as the mean ± SEM (n = 6). Sm int, small intestine; Lg int, large intestine.

injection. The blood concentration peaked at 0.5 h after injection ($1.28 \pm 0.07\%$ ID/g and $0.77 \pm 0.07\%$ ID/g for HA-NPs and HA-polymer, respectively), then dramatically decreased, with the lowest level occurring from 2 h to 6 days after injection. At the peak, HA-NPs showed higher radioactivity than HA-polymers (Fig. 1).

Organ distribution

The organ distribution after intravenous injection of ¹⁷⁷Lu labeled HA-NPs and HA-polymers at 0.5 h, 2 h, 1 day, 3 days, 7 days, 14 days and 28 days after injection is shown Figure 2. The HA radioactivity primarily appeared in the liver, spleen, lung, kidney and heart. The distribution of HA-NPs occurred in the following order (ascending): liver, spleen, lung, kidney, and heart (Fig. 2A). However, the HA-polymers distribution occurred in the following ascending order: spleen, liver, lung, kidney, and heart (Fig. 2B).

In livers, HA-NPs were peak levels ($92.2 \pm 2.74\%$ ID/g) at 1 day after injection, while the peak levels ($103 \pm 2.59\%$ ID/g) of HA-polymers showed at 2 h after injection. Until 28 days after injection, HA-NPs was rapidly decreased to $36.5 \pm$

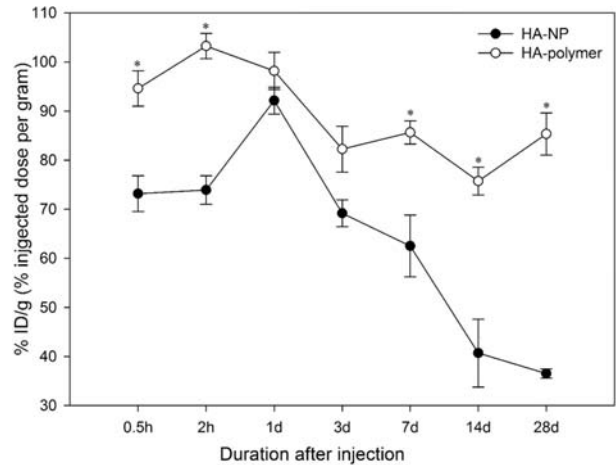


Fig. 3. Biodistribution of ¹⁷⁷Lu-labeled HA-NP (●) and HA-polymers (○) in the livers of ICR mice after intravenous injection at different time periods. The initial HA-NPs and HA-polymers distribution tendency was similar, after which HA-NP distribution showed a steep decline while HA-polymer showed a gradual decline. Data are presented as injected dose per gram (%ID/g) and expressed as the mean ± SEM (n = 6). *p < 0.05 between HA-NPs and HA-polymers.

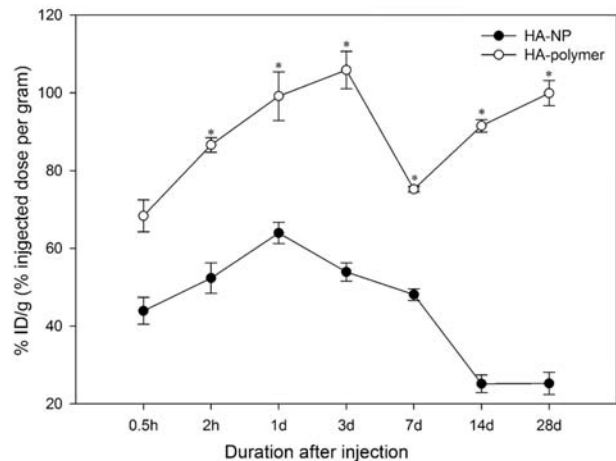


Fig. 4. Biodistribution of ¹⁷⁷Lu-labeled HA-NPs (●) and HA-polymers (○) in the spleens of ICR mice after intravenous injection at different time periods. The results showed that a similar distribution pattern between HA-NP and HA-polymer at 1 day after administration, but that the distribution of HA-polymers was much higher than that of HA-NP. Data are presented as injected dose per gram (%ID/g) and expressed as the mean ± SEM (n = 6). *p < 0.05 between HA-NPs and HA-polymers.

0.94% ID/g, but HA-polymers maintained a high level ($85.35 \pm 4.30\%$ ID/g; Fig. 3).

In spleens, HA-NPs were observed at 1 day after injection ($63.94 \pm 2.75\%$ ID/g), after which they slowly decreased until 14 days. High levels of HA-polymers were observed ($68.37 \pm 4.12\%$ ID/g) at 0.5 h after injection, and at 3 days after injection ($105.87 \pm 4.79\%$ ID/g), while they dramatically

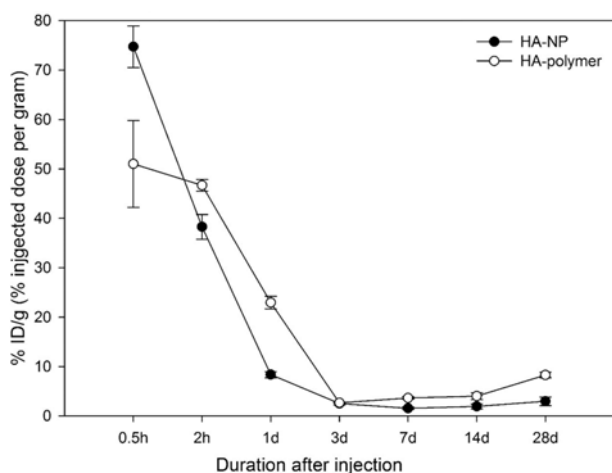


Fig. 5. Biodistribution of ^{177}Lu -labeled HA-NPs (●) and HA-polymers (○) in the lungs of ICR mice after intravenous injection at different time periods. Both HA-NP and HA-polymer levels showed a similar tendency to decrease with time intervals. Data are presented as injected dose per gram (%ID/g) and expressed as the mean \pm SEM (n = 6).

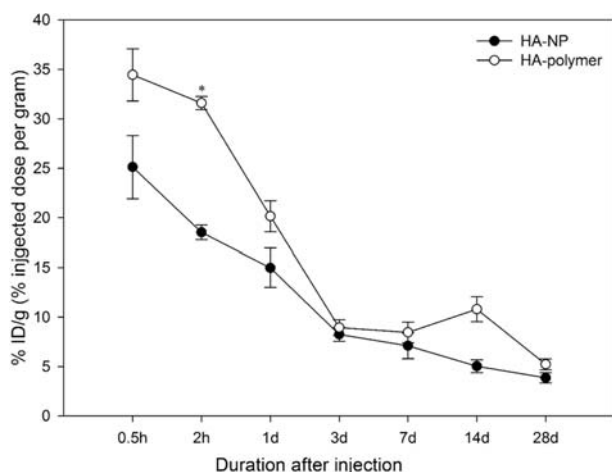


Fig. 6. Biodistribution of ^{177}Lu -labeled HA-NPs (●) and HA-polymers (○) in the kidneys of ICR mice after intravenous injection at different time periods. Both HA-NP and HA-polymer levels showed a similar tendency to decrease with time intervals. Data are presented as injected dose per gram (%ID/g) and expressed as the mean \pm SEM (n = 6). * $p < 0.05$ between HA-NPs and HA-polymers.

decreased at 7 days after injection ($75.22 \pm 0.69\%$ ID/g), then slowly increased again ($99.92 \pm 3.22\%$ ID/g) at 28 days after injection (Fig. 4).

In lungs, both HA-NPs and HA-polymers were taken up dramatically at 0.5 h ($74.72 \pm 4.20\%$ ID/g and $51.01 \pm 8.8\%$ ID/g, respectively), then remarkably decreased after 3 days ($2.51 \pm 0.30\%$ ID/g and $2.65 \pm 0.1\%$ ID/g, respectively), after which they were maintained at low levels (Fig. 5).

In kidneys, both HA-NPs and HA-polymers were taken up

rapidly at 0.5 h after injection ($25.12 \pm 3.10\%$ ID/g and $34.45 \pm 2.64\%$ ID/g, respectively), then sharply decreased at 3 days, after which they were maintained at low levels ($3.68 \pm 0.52\%$ ID/g and $5.22 \pm 0.56\%$ ID/g) until 28 days after injection (Fig. 6).

Discussion

Nanomaterials may show differences in toxicity and bio-distribution depending on size, physical and chemical differences and routes of exposure. Accordingly, it is necessary to fully investigate the safety and toxicological issues associated with using nanoparticles as potential materials of nanomedicine. This study was conducted to determine the distribution and time-dependent fate of HA-NPs or -polymers in the blood and organs of mice following intravenous injection at various time intervals. ^{177}Lu -labeled HA-NPs or HA-polymers were injected into ICR male mice at a dose of 5 mg/kg and the amount of radioactivity remaining in the blood and several target organs was measured from 0.25 h to 28 days.

The radioactivity of ^{177}Lu -labeled HA-NPs and HA-polymers increased at 0.5 h after injection in the blood, then decreased to its lowest level after 2 h, where it remained for 6 days. At its peak, HA-NPs showed the higher radioactivity than HA-polymers. The blood clearance of HA-polymers decreased relative to HA-NPs because HA-polymer is more easily captured by the organs while circulating in the blood. An *in vivo* biodistribution study of mesoporous silica nanoparticles (MSNs) suggested that both large MSNs and polyethylene-glycolated (PEGylated)-MSNs can be more easily captured by the organs. The size of these materials was similar to that of the HA-NPs we used. They considered smaller sized materials to have a longer blood-circulation lifetime, which could reflect the slower capture by various organs [15]. Similarly, gold nanoparticles administered via intravenous injection showed long-term blood circulation. Large nanoparticles showed a shorter blood half-life than small nanoparticles [6]. Moreover, the organ distribution of HA-polymers was higher than that of HA-NPs since HA-polymers are taken up by the organs.

In tissues, HA-NPs and HA-polymers were mainly observed in the liver, spleen, lung, kidney, and heart, but also occurred in smaller levels in other organs. The HA-NPs levels tended to gradually decrease in the liver and spleen, but HA-polymer accumulated until 28 days.

In the liver, the HA-NPs and HA-polymers distribution tendency was different, with HA-NPs distribution showing a steep decline and HA-polymers in a gradual decline. HA-polymers was reached the peak much earlier than HA-NP in their depositions and maintained for a long time, while HA-NP decreased very fast after reaching the peak. The capture rates of HA-polymers by the liver are faster than the degradation rates and excretion rates; therefore, the HA-polymers distribution accumulated. The HA-NPs distribution declined because the degradation rates are higher than the capture

rates. Based on the steep decline of HA-NPs, degradation, and excretion, redistribution is expected to take place actively. Injected nanoparticles directly entered into circulation and the liver via a first-pass effect, after which they were re-distributed from the liver to other organs [6]. Both HA polymers and HA-NPs were observed at high levels in the liver because the hyaluronan receptor for endocytosis (HARE) is abundant in the liver [2]. Significant localization of chlorotoxin-conjugated iron oxide nanoparticles was seen in slices from the tissues of the reticuloendothelial system (RES) in the liver, spleen, and bone marrow, as well as the kidneys. The binding patterns in the liver and spleen suggested macrophage uptake [18]. Several previous studies suggested that higher accumulation in the liver is reasonable because of higher opsonization and macrophage recognition or due to direct recognition by the liver (Kupffer cell receptor-mediated endocytosis). Interestingly, 237 to 424 nm of HA-NPs showed remarkable accumulations in the liver owing to HA-NPs uptake in the phagocytic cells of RES and the hepatic sinusoidal endothelial cells with HARE receptor [7]. The HA-polymers distribution showed an accumulation in the liver since the capture rates are higher than the degradation and excretion rates.

Unlike the liver, the distribution of HA-polymers in the spleen was much higher than that of HA-NPs. HA-NPs showed a mild increasing tendency for up to 1 day after injection, after which they tended to decrease steadily because of the slow, continual degradation. The HA-polymers distribution increased until 3 days after injection, but abruptly decreased at 7 days, after which it increased again until 28 days. The initial increase in HA-polymers appeared to affect continuous capture and accumulation, except an abrupt degradation at 7 days and then, the increasing tendency after 7 days may be caused by the continuous capture and accumulation and decreased degradation rates. An *in vivo* biodistribution study of MSNs to evaluate the effects of particle size and PEGylation indicated that relatively smaller particle size, MSNs-80 nm, PEG-MSNs-80 nm, MSNs-120 nm, and PEG-MSNs-120 nm, the biodistribution of these samples in liver and spleen decreased generally, then increased, and finally decreased again with time post-injection like as the this our results in the liver and spleen injected with HA-NPs. Within 1 month of injection, the biodistribution of PEG-MSNs and MSNs in the liver and spleen decreased again relative to 5 days after injection, which could be due to their slow but continued degradation. These findings also imply that there were always both uncaptured PEG-MSNs and MSNs remaining and circulating in the blood [15]. In the present study, HA-NPs showed a mild increasing tendency for up to 1 day after injection, after which they tended to decrease steadily and were very low after 14 days. The distribution of HA-NPs may be associated with macrophages, which play an important role in the cellular response to particles in the spleen at initial periods after injection, but not at late stages [5]. Similar to the liver, HA-polymer in the spleen

tended to accumulate. These findings indicate that the capture rates of HA-polymer in the spleen, relatively larger particle size than HA-NPs, are higher than the degradation and excretion rates, and that macrophages may play a significant role in the tendency for HA-polymer to accumulate in the spleen, although it is difficult to interpret the sudden decline after 7 days.

In the lung and kidney, both HA-NP and HA-polymer levels showed a similar tendency to decrease with time, probably because their degradation rates were higher than their accumulation rates. The distribution in the lung showed a steeper decrease than in the kidney, likely because HA migrated from other organs to kidney and was then excreted. The distribution in the lung was low from 3 days after injection. A previous study of folate-conjugated shell cross-linked nanoparticles (SCK) indicated that both SCK-folate and SCK exhibited immediate lung uptake, probably because of sequestration of some aggregated nanoparticles by the lung capillary bed after intravenous injection [20]. Different from the liver and spleen, the lung and kidney appeared to have a relatively stable decreasing tendency because there was no accumulation from other organs.

In the heart, HA-NPs decreased almost immediately after injection to a level small enough to make it difficult to determine distribution at 1 day after injection. HA-polymers then rapidly increased shortly after injection, and then showed a similar decreasing distribution as HA-NP after 1 day. This trend in the heart was unexpected and likely reflects an over-estimation of the remaining blood. The blood remaining in the organ is not known. Thus, the observed radioactivity in organs containing large amounts of blood such as kidneys, heart, and liver may be somewhat exaggerated [9].

The blood-testis barrier BTB is a physiological barrier between blood vessels and seminiferous tubules, which prevents cytotoxic substances from entering the seminiferous tubules [1]. Similarly, the blood-brain barrier (BBB) is composed of endothelial cells connected to tight junctions as a barrier with highly selective permeability to prevent external toxic substances from entering the brain in the central nervous system (CNS) [14]. The reason that nanoparticles cannot easily enter the brain is because endothelial cells have tight junction structures without pinocytotic vesicles and fenestrations [4]. In the present study, radioactivity of HA-NPs and HA-polymers in the brain and testis was extremely low. Based on these findings, the HA-NPs and HA-polymers have no capability to penetrate the BBB and BTB and are not accumulated in the brain or testis.

HA-NPs and HA-polymers showed particularly low radioactivity in the gastrointestinal tract when compared with other organs. The maximum radioactivity of HA in this region was observed shortly after injection, after which it steadily decreased. These findings indicate that there is no redistribution or migration of HA-NPs from other organs and also does not charged excretion. Following oral administration, the distribution of NPs in the gastrointestinal tract was strongly detected,

after which it rapidly decreased, likely because of degradation by the acidic stomach medium [17]. In contrast, in the present study, HA biodistribution was low in the gastrointestinal tract because it was administered intravenously and its redistribution and excretion could not be predicted due to the significant change with time.

This pharmacokinetics and organ distribution study was intended to elucidate the size-dependent distribution pattern of HA in mice. However, this study did not evaluate the excretion route and not all relevant pharmacokinetics processes were measured. A temporal study design could indicate the pharmacokinetic half-life of nanoparticles of various sizes. Such a study would provide more information regarding whether the chemical composition or physical characteristics such as the size and shape of the nanoparticles is the main factor influencing *in vivo* distribution [6]. However, we only compared the blood clearance and organ distribution of HA-NPs and HA-polymers after intravenous injection into mice. These findings demonstrated that blood clearance and organ distributions of HA are different depending on particle size. The blood clearance of HA-polymer was decreased compared with that of HA-NP because HA-polymer was more easily captured by the organs while circulating in the blood. Because the blood clearance of HA-NP remained higher, it is reliably excreted without accumulation. HA-polymers could more easily be captured by the liver and spleen, and showed greater accumulation because of the slow biodegradation and low amount of excreted degradation products. This undesirable and higher accumulation in the liver and spleen of HA-polymers should be considered if these compounds are to be used for delivering specific drugs possessing toxicity to the liver and spleen; accordingly, additional studies should be conducted. Unlike the liver and spleen, the lung and kidney showed relatively stable distribution of HA-polymers.

In conclusion, our results suggest that HA-NPs did not accumulate in the liver and spleen, or in the lung, kidney and heart. Overall, this study provides evidence that HA-NPs are selectively distributed but not accumulated into the liver and spleen, implying their potential for use as nanocarriers for diagnosis and therapy.

Acknowledgments

Authors wish to thank Dr. Kwangmeyung Kim of the Korea Institute of Science and Technology who kindly provided HA-polymers and HA-NPs. This research was supported by Basic Science Research Program (2016R1D1A1B01015625) and the Priority Research Centers Program (2015 R1A6A1A04020885) through the National Research Foundation of Korea (NRF) funded by the Ministry of Education, Science and Technology, the grant (09152-nanotoxicity-697) from the Korea Food and Drug Administration, and the research grant of the Chungbuk National University in 2014.

References

1. **Barrett KE, Barman SM, Boitano S, Brooks HL.** Ganong's Review of Medical Physiology. 24 ed. McGraw-Hill, Hong Kong, 2012.
2. **Bharadwaj AG, Kovar JL, Loughman E, Elowsky C, Oakley GG, Simpson MA.** Spontaneous metastasis of prostate cancer is promoted by excess hyaluronan synthesis and processing. *Am J Pathol* 2009, **174**, 1027-1036.
3. **Buzea C, Pacheco II, Robbie K.** Nanomaterials and nanoparticles: sources and toxicity. *Biointerphases* 2007, **2**, MR17-71.
4. **Chertok B, Moffat BA, David AE, Yu F, Bergemann C, Ross BD, Yang VC.** Iron oxide nanoparticles as a drug delivery vehicle for MRI monitored magnetic targeting of brain tumors. *Biomaterials* 2008, **29**, 487-496.
5. **Cho M, Cho WS, Choi M, Kim SJ, Han BS, Kim SH, Kim HO, Sheen YY, Jeong J.** The impact of size on tissue distribution and elimination by single intravenous injection of silica nanoparticles. *Toxicol Lett* 2009, **189**, 177-183.
6. **Cho WS, Cho M, Jeong J, Choi M, Han BS, Shin HS, Hong J, Chung BH, Jeong J, Cho MH.** Size-dependent tissue kinetics of PEG-coated gold nanoparticles. *Toxicol Appl Pharmacol* 2010, **245**, 116-123.
7. **Choi KY, Chung H, Min KH, Yoon HY, Kim K, Park JH, Kwon IC, Jeong SY.** Self-assembled hyaluronic acid nanoparticles for active tumor targeting. *Biomaterials* 2010, **31**, 106-114.
8. **Choi KY, Min KH, Na JH, Choi K, Kim K, Park JH, Kwon IC, Jeong SY.** Self-assembled hyaluronic acid nanoparticles as a potential drug carrier for cancer therapy: synthesis, characterization, and *in vivo* biodistribution. *J Mater Chem* 2009, **19**, 4102-4107.
9. **De Jong WH, Borm PJ.** Drug delivery and nanoparticles: applications and hazards. *Int J Nanomedicine* 2008, **3**, 133-149.
10. **De Jong WH, Hagens WI, Krystek P, Burger MC, Sips AJAM, Geertsma RE.** Particle size-dependent organ distribution of gold nanoparticles after intravenous administration. *Biomaterials* 2008, **29**, 1912-1919.
11. **Falcone SJ, Palmeri DM, Berg RA.** Rheological and cohesive properties of hyaluronic acid. *J Biomed Mater Res A* 2006, **76**, 721-728.
12. **Fraser JRE, Laurent TC, Laurent UBG.** Hyaluronan: its nature, distribution, functions and turnover. *J Intern Med* 1997, **242**, 27-33.
13. **Han SY, Han HS, Lee SC, Kang YM, Kim IS, Park JH.** Mineralized hyaluronic acid nanoparticles as a robust drug carrier. *J Mater Chem* 2011, **21**, 7996-8001.
14. **Hawkins BT, Davis TP.** The blood-brain barrier/neurovascular unit in health and disease. *Pharmacol Rev* 2005, **57**, 173-185.
15. **He Q, Zhang Z, Gao F, Li Y, Shi J.** In vivo biodistribution and urinary excretion of mesoporous silica nanoparticles: effects of particle size and PEGylation. *Small* 2011, **7**, 271-280.
16. **Koo H, Huh MS, Ryu JH, Lee DE, Sun IC, Choi K, Kim K, Kwon IC.** Nanoprobes for biomedical imaging in living systems. *Nano Today* 2011, **6**, 204-220.
17. **Laznick M, Laznickova A, Cozikova D, Velebný V.** Preclinical pharmacokinetics of radiolabelled hyaluronan.

- Pharmacol Rep 2012, **64**, 428-437.
18. **Lee MJ, Veiseh O, Bhattarai N, Sun C, Hansen SJ, Ditzler S, Knoblaugh S, Lee D, Ellenbogen R, Zhang M, Olson JM.** Rapid pharmacokinetic and biodistribution studies using chlorotoxin-conjugated iron oxide nanoparticles: a novel non-radioactive method. PLoS One 2010, **5**, e9536.
 19. **Peer D, Karp JM, Hong S, Farokhzad OC, Margalit R, Langer R.** Nanocarriers as an emerging platform for cancer therapy. Nat Nanotechnol 2007, **2**, 751-760.
 20. **Rossin R, Pan D, Qi K, Turner JL, Sun X, Wooley KL, Welch MJ.** ⁶⁴Cu-labeled folate-conjugated shell cross-linked nanoparticles for tumor imaging and radiotherapy: synthesis, radiolabeling, and biologic evaluation. J Nucl Med 2005, **46**, 1210-1218.
 21. **Saini R, Saini S, Sharma S.** Nanotechnology: the future medicine. J Cutan Aesthet Surg 2010, **3**, 32-33.